





Quantifying land degradation in the Zoige Basin, NE Tibetan Plateau using satellite remote sensing data

YU Kai-feng *  <http://orcid.org/0000-0001-5434-1386>;  e-mail: kaifeng.yu@geo.rwth-aachen.de

Frank LEHMKUHL  <http://orcid.org/0000-0002-6876-7377>; e-mail: flehmkuhl@geo.rwth-aachen.de

Dimitri FALK  <http://orcid.org/0000-0002-7071-1073>; e-mail: dimitri.falk@geo.rwth-aachen.de

* Corresponding author

Department of Geography, RWTH Aachen University, Templergraben 55, 52056 Aachen, Germany

Citation: Yu KF, Lehmkühl F, Falk D (2017) Quantifying land degradation in the Zoige Basin, NE Tibetan Plateau using satellite remote sensing data. *Journal of Mountain Science* 14(1). DOI: 10.1007/s11629-016-3929-z

© Science Press and Institute of Mountain Hazards and Environment, CAS and Springer-Verlag Berlin Heidelberg 2017

Abstract: Considerable efforts have been dedicated to desertification research in the arid and semi-arid drylands of central Asia. However, there are few quantitative studies in conjunction with proper qualitative evaluation concerning land degradation and aeolian activity in the alpine realm. In this study, spectral information from two Landsat-5 TM scenes (04.08.1994 and 28.07.2009, respectively) was combined with reference information obtained in the field to run supervised classifications of eight landscape types for both time steps. Subsequently, the temporal and spatial patterns of the alpine wetlands/grasslands evolutions in the Zoige Basin were quantified and assessed based on these two classification maps. The most conspicuous change is the sharp increase of ~627 km² degraded meadow. Concerning other land-covers, shallow wetland increases ~107 km² and aeolian sediments (mobile dunes and sand sheets) have an increase of ~30 km². Considering the deterioration, an obvious decrease of ~440 km² degraded wetland can be observed. Likewise, decrease of deep wetland (~78 km²), humid meadow (~80 km²) and undisturbed meadow (~88 km²) were determined. These entire evolution matrixes undoubtedly hint a deteriorating tendency of the Zoige Basin ecosystem, which is characterized by significantly declined proportion of intact wetlands, meadow, rangeland and a considerable increase of

degraded meadow and larger areas of mobile dunes. In particular, not only temporal alteration of the land-cover categories, the spatial and topographical characteristics of the land degradation also deserves more attention. In the alpine rangelands, the higher terraces of the river channels along with their slopes are more liable to the degradation and desertification. This tendency has significantly impeded the nomadic and agriculture activities. The set of anthropo-zoogenic factors encompassing enclosures, overgrazing and trampling, rodent damaging and exceedingly ditching in the wetlands are assumed to be the main controlling mechanisms for the landscape degradation. A suite of strict protection policies is urgent and indispensable for self-regulation and restoration of the alpine meadow ecosystem. Controlling the size of livestock, less ditching in the rangeland, and the launching of a more strict nature reserve management by adjacent Ruergai, Maqu and Hongyuan Counties would be practical and efficacious in achieving these objectives.

Keywords: Alpine ecosystem; Wetlands; Degradation; Desertification; Zoige Basin; Driving mechanisms

Introduction

Desertification and landscape evolution

Received: 6 March 2016
Revised: 27 March 2016
Accepted: 21 July 2016

accompanied by possible driving mechanisms of sandy fields in arid central Asia (e.g. northern China) were intensively studied over decades (Zhu et al. 1988; Lu et al. 2013; Yu et al. 2013, 2016). Less effort, however, has been dedicated to the relative high-moisture alpine realm. Lehmkuhl et al. (2003) suggest a successive geomorphological section in the arid central Asia from higher Khangai Mountain to the Gobi Desert, Badain Jarain Desert, Qilian Mountain, Qaidam Basin and eventually to the NE Tibet. According to climatic and topographic settings, this section covers a holistic array of geomorphic units including glacial and periglacial land forms, pediments/bajadas, steppe and desert gorges, aeolian landforms and floodplain valleys with meandering rivers. Interestingly, although the mean annual precipitation is greater than 600 mm and restoration policies have been carried out since the 1990s, at the southern end of the section i.e. NE Tibet (Zoige Basin), huge amounts of mobile dunes or sand sheets can be observed (Lehmkuhl 1993, 1995, 1997; Lehmkuhl and Liu 1994; Meinert and Gudehus 2013). In Zoige Basin, in the context of present moisture supply, at least fixed dunes with vegetation development would be expected (Lehmkuhl and Liu 1994). However, as investigated by Lehmkuhl (1993, 1997), the desertification process in the Zoige Basin started in the late 1970s, the area was completely covered with grass and peat bogs since the beginning of the 20th century. Furthermore, the phase between 1980s and 2000s is suggested as the primary desertification period in the Zoige Basin (Hu et al. 2015).

The Zoige Basin is regarded as one of the biggest alpine plateau-type wetland of the world and the largest peat storage in China, in which ~5.54 pg carbon are stored (XJ Guo et al. 2013). Located around the headwaters of Yellow River (Figure 1), rapid rangeland degradation, drying of wetlands, as well as dune accumulation in the drainage basin are threatening Asia's main water supply (Qiu 2016). In addition, both the topogenous and soligenous wetland, which serves as a carbon sink and source of methane, of the Zoige Basin might also strengthen the greenhouse effect and contribute to global climate change (Du et al. 2004; Chen et al. 2009; Charman et al. 2013; Zhao et al. 2014). Previously, only a few studies

have been conducted concerning the quantitative analysis of the landscape evolution in this alpine realm (Lehmkuhl 1997; Zeng et al. 2003; Dong et al. 2010; Pang et al. 2010; Bai et al. 2013; Hu et al. 2015; Li et al. 2015). A holistic evolution matrix comprising a whole set of land-covers together with consideration of accuracy assessment is of particular importance in order to gain complete knowledge of land degradation and desertification in this alpine realm. Thus, quantitative analysis of the landscape evolution using satellite imagery data along with reference information obtained in the field is a substantial step to estimate the potential interplays between the alpine ecosystem and the potential driving factors, thereby providing a robust dataset for the policy makers (cf. Harris 2010).

In this study, the above issue is addressed by conducting a post-classification change analysis based on two Landsat-5 scenes (August 1994 and July 2009) acquired over the Zoige Basin. These dates were selected for the following reasons: (i) year 1994 was the inception of the Zoige Marsh Nature Reserve launched by the government (Xiang et al. 2009); (ii) the years between 2007 and 2010 were the onset of newly announced policies against the artificial drainage in the Zoige rangeland (Hu et al. 2015); and (iii) since around 2010, based on our field investigations, no further conspicuous degradation processes can be observed, which may result from lately launched preserving strategies.

We performed a quantitative analysis of the landscape evolution between 1994 and 2009 using supervised classification, from which - for the first time in the alpine Zoige rangeland - a quality-evaluated matrix of spatial characteristics of landscape evolution is acquired. Eventually, based on an assessment of climate parameters and number of livestock through those years, possible underlying mechanisms for land degradation and corresponding mitigation strategies are postulated.

1 Study Area

The Zoige Basin is a low-relief plateau located in the northeastern part of Qinghai-Tibet Plateau (32°20'-34°00'N, 101°30'-103°30'E). It covers an area of 26,480 km² with elevation ranges from 3400

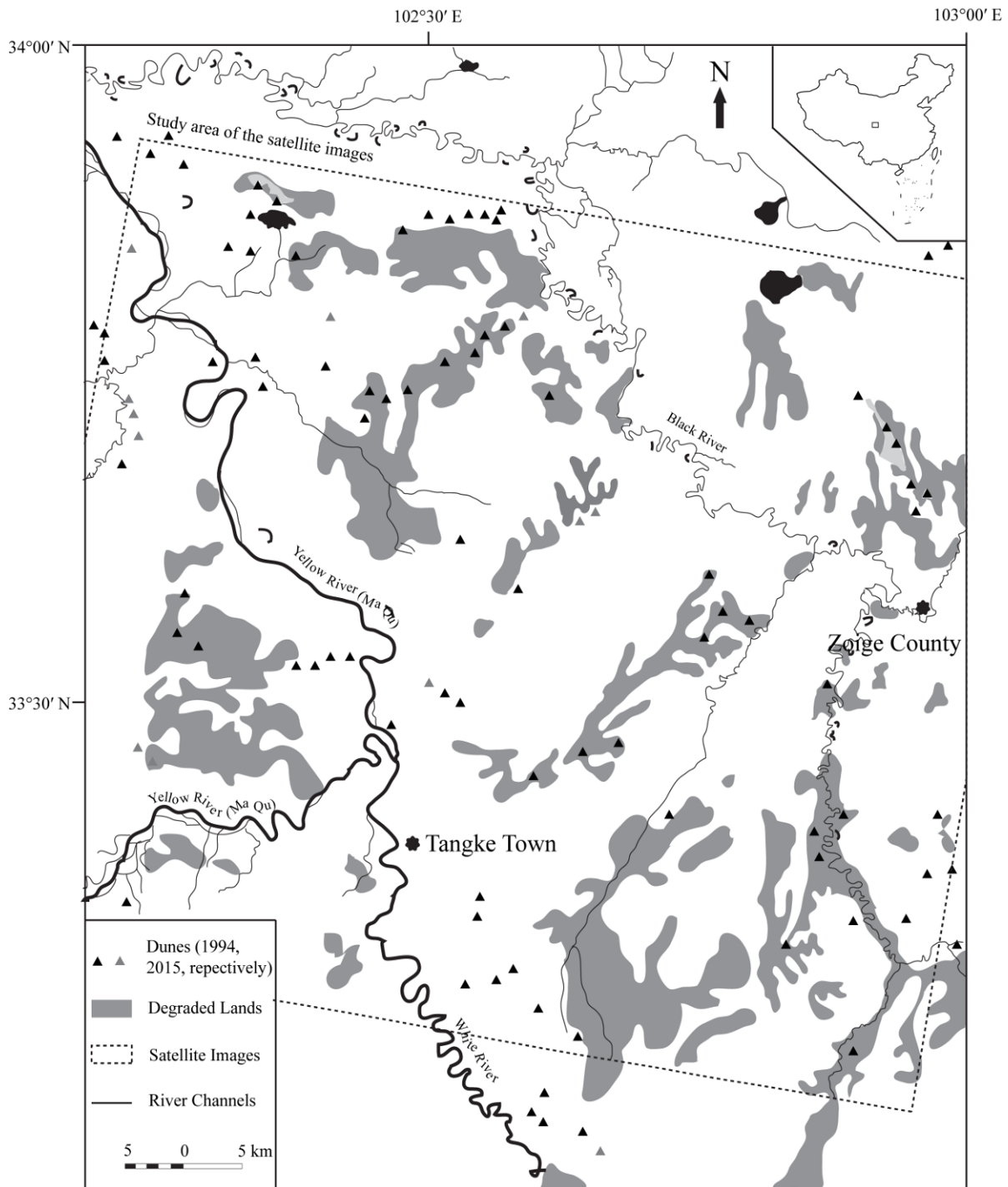


Figure 1 Schematic map of degraded lands and dunes in investigation area in the Zoige Basin. Yellow River flows into the Zoige Basin from west to east and meanders following zigzag pattern towards north. The analyzed satellite image is marked as dashed rectangle. 204 training sites are homogeneously selected throughout the study area. Corresponding coordinates for those sites refer to the supplementary material of this paper.

m to 3700 m above sea level (asl) (Figure 1). The study area borders the provinces of Gansu, Qinghai, and Sichuan, China. The basin lies mainly in the Aba autonomous prefecture encompassing Zoige County,

Hongyuan County, Aba County and Maqu County. The Anyemaqen Mountain Range is located to the east of the basin, along with Min Mountain and Qionglai Mountain to the south and west.

1.1 Climatic setting

In the Zoige Basin, mean annual precipitation is as high as 654 mm, allowing the growth of alpine meadow and even patches of forest on northern slopes (Lehmkuhl and Liu 1994). Eighty-five percent of precipitation is delivered from April to September and over half (ca. 52%) from June to August. The basin is affected partially by annual westerlies and the cold arid winter monsoon (Cui and Graf 2009). Local orographic configurations may also affect the regional wind patterns and humid-thermal regimes. In general, gradual transition from cold-arid in the northwest to warm-humid climate in the southeast can be observed (Du 1996). During summer, this region is within the reach of the generally warm-humid East Asian Summer Monsoon (EASM) while the controlling atmospheric cycling system in winter is the arid-cold and windy NW winter monsoon (Chen et al. 1999). Thus, the modern climate is marked by a short monsoonal humid summer and long arid winter (Dong et al. 2010), which is corresponding to the subarctic (boreal) climate in the Köppen classification system (Kottek et al. 2006). The mean annual air temperature is 1.1°C, mean January air temperature is -10.1°C while mean July air temperature is 10.7°C.

1.2 Geologic and geomorphic setting

The Zoige Basin locates along the Songpan-Ganze Terrane that lies south of the Anyaqaen-Kunlun-Muztagh Structure (O'Brian 2001). The bedrock is dominated by intensively deformed Triassic-Jurassic sandstone (Dewey et al. 1988;

Lehmkuhl 1997). In general, the Zoige Basin can be regarded as a pull-apart basin (Lehmkuhl and Spönemann 1994). The basin was occupied by a large lake before 40 ka BP, and covered widely with Holocene peat bogs (Chen et al. 1999). In alpine realm, landscape evolutions are intimately coherent to geomorphological settings, and our literature reviews determined those geomorphic factors had been previously virtually ignored and therefore deserve more attention when attempting to interpret the alpine landscape evolutions. In the Zoige Basin, the wetlands are located along the Black River, the White River, and their tributaries (Figures 1 and 2). Up to 3 m fluvial terrace can be observed by the Yellow River, together with aeolian sediments deposited on the slopes (Lehmkuhl 1997). The dunes and sand sheets are generally stretched in NW-SE direction on the higher terraces of Yellow River and on the slopes of surrounding bedrocks (Figures 3 and 4). Further away from the terraces, meadow, marsh, peat bogs, solifluction features along with frequently occurring land degradation can be observed (Figure 5). In the Zoige Basin, the degradation and desertification of alpine grasslands and wetlands occurred mainly on west-oriented slopes and on the top of hummocks (Lehmkuhl 1997; Figure 1), albeit in some other regions of the eastern Tibetan Plateau, no significant correlation has been detected between the degraded areas and specific slopes or aspects (Fassnacht et al. 2015).

1.3 Vegetation and pedologic setting

Dominant soils in the Zoige Basin are leptosols and regosols together with podzols in dryer areas,



Figure 2 Panoramic photography of the Yellow River north of the settlement of Tangke. View upstream with terrace on the left and floodplain on the right bank (photo: F. Lehmkuhl).

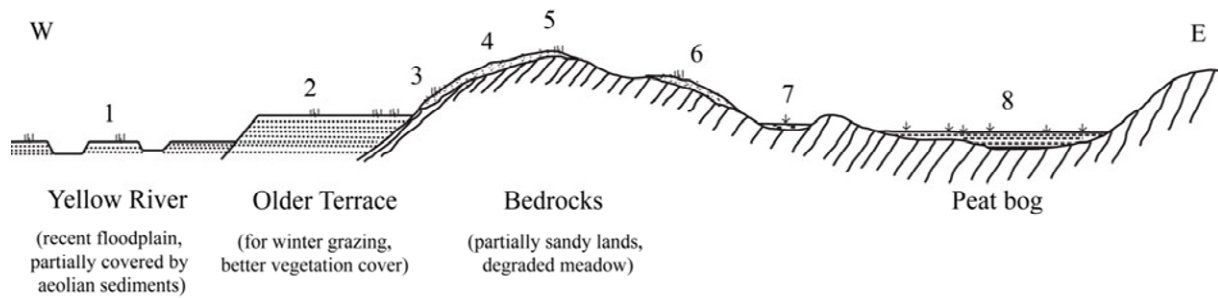


Figure 3 Schematic geomorphic cross section with (geo) ecological land-use pattern in the Zoige Basin (adapted after Lehmkuhl 1997). 1: Recent floodplain covered partially by aeolian sediments. 2: Intact meadow on the higher terraces of Yellow River (for winter grazing). 3: Intact meadow on the river-oriented slopes (for winter grazing). 4: Degraded meadow on the mountains (for summer grazing). 5: Intensively degraded meadow (for summer grazing). 6: Degraded meadow on the east-oriented slopes (for summer grazing). 7: Peat-bogs in the small depressions (for winter grazing). 8: Deeper peat-bogs in the drainage basin.

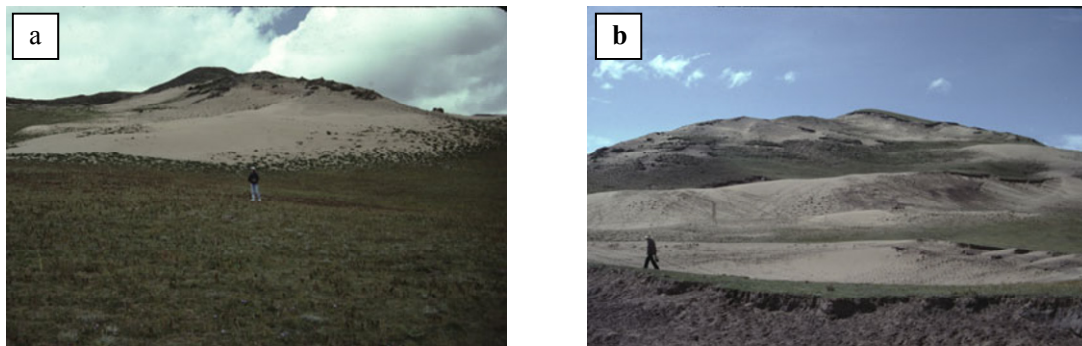


Figure 4 Sandy lands in the Zoige Basin. a: Dunes on the slopes. b: Sand sheets in the lower lands together with dunes on the slopes (photos: F. Lehmkuhl).



Figure 5 Degraded meadow in conjunction with sandy lands in the Zoige Basin. a: Degraded alpine meadow. b: Meadow destroyed by grazing yaks. c: Foot-slope of sand sheets along with fluvial redeposition (photos: F. Lehmkuhl).

while histosol can be observed in vicinity of peat bogs and marsh (Lehmkuhl 1993; Bai et al. 2013). Wetlands in the region are subject to severe ground water decline, inducing the acceleration of peat degradation and carbon emission (Xiang et al. 2009; Guo et al. 2013). In this alpine realm, over 200 genera from 50 families of wetland/grassland taxa were previously identified: *Kobresia pygmaea*, *K. tibetica*, *K. capillifolia*, *K. setchwanensis*, *K. humilis*, *Carex muliensis*, *C. meyeriana*, *C. lasiocarpa*, *C. crebra*, *C. angustifrustrus*, *C. atrata*,

Elymus sibiricus, *E. nutans*, *Deyeuxia scabrecens* and *Deschampsia cespitosa* (Lehmkuhl 1993). Considering arboreal taxa, patches of *Picea* can be sporadically observed on north-exposed slopes up to ~3800 m asl (Lehmkuhl 1997).

1.4 Anthro-po-zoogenic setting

The first signs of nomadic presence in the Zoige Basin were reported to be as early as 7200 cal a BP (cal a BP = calibrated calendar years

before present where “present” is defined as AD 1950; [Schlütz and Lehmkuhl 2009](#)). The “Nomadic Anthropocene” was postulated by [Miehe et al. \(2014\)](#) for the last 6000 years when nomads transformed the natural steppe-like vegetation into *K. pygmaea* pasture. In modern times, with a density of ca. 4.5 people per square kilometer ([Du 1996](#)), human activities play a vital role in altering wetland landscape patterns ([Bai et al. 2013](#)). Landforms become more heterogeneous due to fragmentation of the rangelands ([Figure 6](#)). [Pang et al. \(2010\)](#) reported an area of 410.93 km² of wetlands converted into grassland, which was ascribed to the ditching for pastoralism enlargement launched by the Zoige County. In 1905, the first western explorer A. Tafel visited the area and reported that there were no livestock and grass covered dunes rise above endless peat bogs ([Tafel 1914](#)). However, since the 1960s, significant increased amounts of Yaks, sheep and horses might have triggered the degradation and desertification in this area ([Lehmkuhl 1993; Figure 6](#)).

2 Methodology

The Landsat-5 TM imagery data provides image data with eight-bit radiometric resolution in seven bands comprising the visible, near infrared, shortwave infrared and thermal fractions of the electromagnetic spectrum ([Albertz 2001; Purkis and Klemas 2011](#)). Spectral information of these scenes (04.08.1994 and 28.07.2009, respectively) in conjunction with reference information obtained in the field was employed to run supervised classifications of eight landscape types for both time steps. In addition, these two scenes were selected from summer time with close dates, to reduce the potential impacts of phenology.

Subsequently, the temporal and spatial patterns of landscape evolutions were analyzed based on the two obtained classification maps. A Digital-Globe Quickbird scene (i.e. reference classes) obtained in summer 2009 was integrated with the Google-Earth Maps and was applied thereafter to evaluate the accuracy of the assigned classes (georeferenced positions and matrix refer to the supplementary material of this paper). The routine calculations of producer’s accuracy, user’s accuracy and kappa-coefficient were computed as given in Congalton and [Green \(2008\)](#) and [Lillesand et al. \(2008\)](#). The processing and output of mapping were carried out using ArcGIS 10.1 together with Focus Geomatica 2013 software.

2.1 Priori-identified landscapes and corresponding spectral characteristics

An array of priori-identified landscapes is obtained in the field before the supervised classification. The main classes of geomorphic context in the Zoige Basin are described by [Lehmkuhl \(1993, 1997\)](#) as follows ([Figure 3](#)): (i) recent floodplain on the lower terrace (< 3 m) of Yellow River, which is partially covered by aeolian sediments; (ii) undisturbed (intact) meadow on the higher terrace (8 - 12 m) of Yellow River; (iii) (degraded-) meadow on west-oriented slope; (iv) degraded meadow on the western-exposed slopes; (v) intensively degraded meadow on the hummocks; (vi) degraded meadow on the east-exposed slopes; (vii) shallow emergent marsh (peat-bogs) in the sporadically distributed depressions; and (viii) deeper lentic marsh in the lower lands. Together with towns and agricultural lands, this entire set of classes with assigned category names has allowed us to set up discrete classes, serving as reference pixels in training sites (training area is marked



Figure 6 Livestock influenced alpine meadow and wetlands in the Zoige Basin. a: Alpine meadow and wetlands with surrounding mountains in the background. b: Yaks in the degraded alpine meadow. c: Degraded wetlands due to livestock breeding (photos: F. Lehmkuhl).

with dashed line in Figure 1; detailed georeferenced positions and matrix refer to the supplementary material).

In the context of spectral response signals, different categories are observed in this study. Considering the vegetation, the pronounced absorption of visible lights $0.45\ \mu\text{m}$ and $0.67\ \mu\text{m}$ is contributed to the leaf pigments in parenchyma e.g. chlorophyll (Purkis and Klemas 2011). In the context of natural environment, most of the vegetation denotes green color, absorptions ranges between $0.7\text{-}1.3\ \mu\text{m}$ (Lillesand et al. 2008). Regarding soil, typical absorption spectral ranges from $0.4\ \mu\text{m}$ to $2.5\ \mu\text{m}$ (Richards and Jia 2006), which is depended on the pedogenic intensity, soil wetness, granulometric composition, mineralogical composition and the organic material abundance in the soil (Lillesand et al. 2008). For the water surface, due to the more influencing factors e.g. depth of water and abundance/type of suspension materials, the spectral signals are more complicate compared with preceding landscapes (Albertz 2001). Generally, the distinct absorption occurs at $0.58\ \mu\text{m}$ along with $0.8\ \mu\text{m}$ (Richards and Jia 2006). This whole set of spectral characteristics aids thereafter the accuracy assessment of the classifications (Figure 1).

2.2 Training sites, separability and accuracy evaluations

Training areas near the confluence region of Yellow River and White River along with the priori-identified classes in Section 3.1 are employed to run supervised classifications. The field locations to gather reference information (with coordinates determined by Global Positioning System/GPS equipment) were well distributed throughout the study area (Figure 1). Among the 204 reference locations for each scene, aeolian sediments (3 pixels; 2 pixels), agricultural lands (2 pixels; 3 pixels), deep wetlands (7 pixels; 2 pixels), degraded meadow (24 pixels; 40 pixels), degraded wetlands (21 pixels; 8 pixels), fluvial sediments (4 pixels; 0 pixels), humid meadow (32 pixels; 27 pixels), lake (1 pixels; 7 pixels), meadow (16 pixels; 12 pixels), river (5 pixels; 6 pixels), semi-degraded meadow (76 pixels; 78 pixels), and shallow wetlands (13 pixels; 19 pixels) were acquired in the 1994 and 2009 scene, respectively (Figure 1; georeferenced

positions and matrix refer to the supplementary material). The spectral response curve for each pixel in the training area is generated. Maximum-likelihood algorithm in conjunction with the proceeding spectral characteristics was employed to label and assign each pixel into specific abovementioned classes (Richards and Jia 2006; Mayaux et al. 2008). A significant level of 95% was tested for each pixel, and those pixels did not pass the significance test were regarded as unlabeled (no using) type.

To evaluate the separability of the land-cover classes, the Bhattacharyya-distance of 204 georeferenced positions in the training sites was computed (Schowengerdt 2007; Table 1 for 1994 scene and Table 2 for 2009 scene, respectively). Generally, the larger the Bhattacharyya-distance, the better these two land-covers are distinguished (Lillesand et al. 2008). The value for the distance ranges from 0 to 2, of which larger than 1.8 can be regarded as a well distinguished landscape and -1 is error for interpretation (Mayaux et al. 2008). On the other hand, to further ensure the accuracy of the classifications, the correct assignment of each pixel to one of the considered landscape classes was carried out by comparison with the Digital-Globe Quickbird imagery data (i.e. reference classes). Subsequently, the accuracy percentages are illustrated (Table 3), where values between 0.40 and 0.80 represents moderate agreement and those values greater than 0.80 denote high accuracy of the classifications (Congalton and Green 2008).

3 Results

3.1 Visualization and classification of landscapes in the Zoige Basin

Supervised classification of two Landsat-5 TM scenes captured in 04.08.1994 and 28.07.2009 were carried out (Figure 7), enabling us to quantitatively calculate the temporal and spatial landform evolution from 1994 to 2009 (Table 4; Figures 8 and 9). Apart from the above temporal evolution, a better understanding of the spatial changes of landforms is also indispensable to figure out the possible underlying mechanisms. The changed and unchanged distribution of each

Table 1 Bhattacharyya-distant between different classes (04.08.1994 scene). Low values of separability discussed in the main text are marked in boldface.

	Null	Lake	River	Deep wetland	Shallow wetland	Degraded wetland	Humid meadow	Meadow	Semi-degraded meadow	Degraded meadow	No using	Aeolian	Fluvial	Street	Town
Lake	-1.00	-													
River	-1.00	1.88	-												
Deep wetland	-1.00	2.00	1.97	-											
Shallow wetland	-1.00	2.00	1.99	1.82	-										
Degraded wetland	-1.00	2.00	2.00	2.00	1.93	-									
Humid meadow	-1.00	2.00	2.00	2.00	1.85	1.86	-								
Meadow	-1.00	2.00	2.00	2.00	2.00	2.00	2.00	-							
Semi-degraded meadow	-1.00	2.00	2.00	2.00	2.00	1.99	1.95	1.62	-						
Degraded meadow	-1.00	2.00	2.00	2.00	2.00	1.86	1.99	2.00	1.93	-					
No using	-1.00	2.00	2.00	2.00	2.00	2.00	2.00	1.99	1.98	2.00	-				
Aeolian	-1.00	2.00	2.00	2.00	2.00	2.00	2.00	2.00	2.00	1.98	2.00	-			
Fluvial	-1.00	2.00	1.99	2.00	1.99	1.96	2.00	2.00	2.00	2.00	2.00	1.82	-		
Street	-1.00	2.00	2.00	2.00	2.00	1.98	1.82	1.82	1.43	1.87	1.95	1.96	1.99	-	
Town	-1.00	2.00	2.00	2.00	2.00	1.99	2.00	2.00	1.99	1.97	2.00	1.50	1.38	1.80	-

Table 2 Bhattacharyya-distant between different classes (28.07.2009 scene). Low values of separability discussed in the main text are marked in boldface.

	Null	Lake	River	Deep wetland	Shallow wetland	Degraded wetland	Humid Meadow	Meadow	Semi-degraded Meadow	Degraded Meadow	No using	Aeolian	Fluvial	Street	Town
Lake	-1.00	-													
River	-1.00	1.99	-												
Deep wetland	-1.00	1.97	1.98	-											
Shallow wetland	-1.00	2.00	1.99	1.92	-										
Degraded wetland	-1.00	2.00	2.00	2.00	2.00	-									
Humid Meadow	-1.00	2.00	2.00	2.00	1.99	1.95	-								
Meadow	-1.00	2.00	2.00	2.00	2.00	2.00	2.00	-							
Semi-degraded Meadow	-1.00	2.00	2.00	2.00	2.00	2.00	1.87	1.71	-						
Degraded Meadow	-1.00	2.00	2.00	2.00	2.00	1.96	1.97	1.99	1.75	-					
No using	-1.00	2.00	2.00	2.00	2.00	2.00	2.00	2.00	2.00	2.00	-				
Aeolian	-1.00	2.00	2.00	2.00	2.00	2.00	2.00	2.00	2.00	1.97	2.00	-			
Fluvial	-1.00	2.00	2.00	2.00	2.00	1.98	1.99	2.00	2.00	1.97	2.00	1.11	-		
Street	-1.00	2.00	2.00	2.00	2.00	2.00	1.99	1.93	1.73	1.79	2.00	1.87	1.85	-	
Town	-1.00	2.00	2.00	2.00	2.00	1.98	2.00	2.00	2.00	1.98	2.00	1.54	1.52	1.95	-

Table 3 Accuracy assessment for each landscape based on the comparison between the assigned classes and the reference classes.

Landscape	1994*			2009*		
	Producer's accuracy/%	User's accuracy/%	Kappa-coefficient	Producer's accuracy/%	User's accuracy/%	Kappa-coefficient
Lake	100.00	50.00	0.50	100.00	100.00	1.00
River	80.00	100.00	1.00	100.00	100.00	1.00
Deep wetland	85.71	85.71	0.85	100.00	40.00	0.39
Shallow wetland	84.62	73.33	0.72	73.68	73.68	0.71
Degraded wetland	71.43	68.18	0.65	75.00	75.00	0.74
Humid meadow	81.25	89.66	0.88	77.78	84.00	0.82
Undisturbed meadow	93.75	79.95	0.77	91.67	68.75	0.67
Semi-degraded meadow	86.84	92.96	0.89	84.62	92.96	0.89
Degraded meadow	79.71	82.61	0.80	82.50	84.62	0.81
Agriculture lands	100.00	50.00	0.50	100.00	100.00	1.00
Aeolian sediments	100.00	75.00	0.75	100.00	40.00	0.39
Fluvial Sediments	75.00	75.00	0.75	-	-	-

Notes: *The inventory of georeferenced positions are listed in the supplementary material. The 204 field locations to gather reference information were well distributed throughout the study area from both 1994 and 2009 scene, respectively. More details concerning the calculations of the producer's accuracy, user's accuracy and kappa-coefficient refer to Congalton and Green (2008) and Lillesand et al. (2008).

landscape is visualized in Figure 9. The undisturbed meadow is the dominant landscape on the terraces of Yellow River and gradually changes to semi-degraded meadow further away from the channels. Sporadic distribution of dunes can be observed on the terraces of White River and Black River. Areas adjacent to wetland/peat bogs are generally occupied by humid meadow.

3.2 Quality evaluation as inferred from the reference pixels

High separability of the classes is illustrated by the general high values of 2.00 between most of the land-covers (Table 2). In the 04.08.1994 scene, relatively low statistical distances of 1.62 (semi-degraded meadow/meadow), 1.50 (town/aeolian sediments), 1.43 (street/semi-degraded meadow) and 1.38 (town/fluvial sediments) occur, indicating a major confusion between these set of classes. These statistically unseparated landscapes (in particular <1.8) may be ascribed to the insufficient spectral and/or spatial resolution of the TM images. For the 28.07.2009 scene, most statistical distance between land-covers is 2.00 (Table 2), implying that the separability of the landscapes categories is generally acceptable. Relatively low values occur only between semi-degraded meadow/meadow (1.71), semi-degraded meadow/degraded meadow (1.75), semi-degraded meadow/street (1.73), degraded meadow/street (1.79), fluvial/aeolian sediment (1.11), town/fluvial sediment (1.45), and aeolian/fluvial sediment (1.52), suggesting

relatively lower separability for these land-covers. On the other hand, the overall accuracy of both 1994 and 2009 scenes are generally larger than 80.00% (Table 3), implying that the classification has a sufficient performance for subsequent temporal and spatial analyses. In particular, relatively low accuracy (i.e. <0.50) only occurs to the lake and agriculture land landscapes/classes in the 1994 scene and deep wetland and aeolian sediments classes in the 2009 scene (Table 3).

4 Discussion

In the light of the generally high performance of separability and accuracy of the classifications (Tables 1, 2 and 3), further discussions concerning temporal and spatial characteristics of the land evolutions are permitted. However, with respect to specific land-over type e.g. agriculture lands in 1994 scene, aeolian sediments and deep wetland in 2009 scene (Table 3), the merely moderate accuracy may hamper any further explanations, leaving us to evaluate the temporal and spatial patterns rather based on a more holistic land-cover evolution matrix as in Table 4, instead of considering only single land-cover such as aeolian sediments or deep wetland. Furthermore, land-covers, e.g. river, fluvial sediments and townships, which may be readily influenced by phenological/meteorological factors and settlement planning, are excluded from the following discussions.

4.1 Temporal and spatial characteristics of landscape evolution in the Zoige Basin

4.1.1 Temporal characteristics of landscape evolution

Comparing the 1994 and 2009 scenes (Figure 7), the lower terraces of the Yellow River are dominated by intact/undisturbed meadow and semi-degraded meadow (Table 4). NW-stretched

dune fields are sporadically detected on the eastern and western flanks of higher terraces. According to Lehmkühl (1997), this may be generated from the fluvial sediment which is exposed during dry periods or winter times. On the slopes of terraces, especially near the confluence of the tributary White River into the Yellow River (Figure 1), large areas of intact/semi-degraded meadow and agriculture land are converted into degraded,

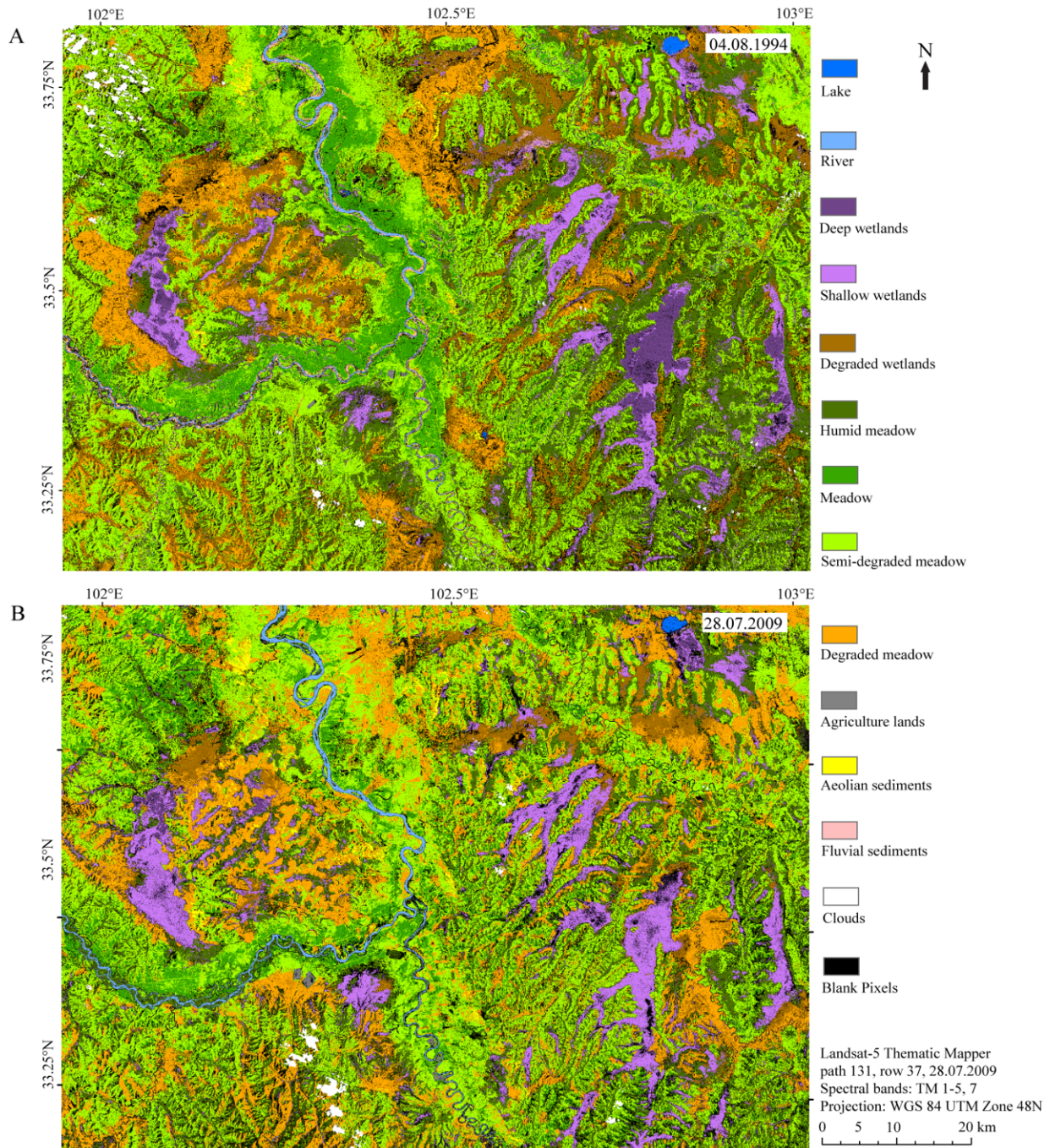


Figure 7 Classification of the Landsat-5 TM scene as determined by the supervised classification. Panel A denotes the 04.08.1994 scene, and panel B represents the 28.07.2009 scene.

Table 4 Sequential evolution matrix for each landscape (Unit: km²). Significant values discussed in the main text are marked in boldface*.

1994	2009												
	Lake	River	Deep wetland	Shallow wetland	Degraded wetland	Humid Meadow	Meadow	Semi-degraded Meadow	Degraded Meadow	Town	Aeolian	Fluvial	
Lake	4.29	0.37	0.08	0.04	0	0.03	0	0.01	0.01	0	0	0	
River	0.12	32.75	0.04	0.16	0.03	0.66	0	0.06	0.03	0	0.02	0	
Deep wetland	0	0	3.57	70.99	4.92	0.41	0	0.03	0.05	0	0	0	
Shallow wetland	0.01	0.70	8.71	198.52	55.41	40.54	1.85	21.31	7.79	0	0.20	0	
Degraded wetland	0	0.15	1.54	70.65	57.81	205.77	1.66	104.56	54.61	0	0.84	0	
Humid Meadow	0	0.07	0.23	98.30	38.78	47.04	5.82	169.36	59.12	0	0.16	0	
Meadow	0	0.23	0	0.08	0.07	1.34	178.13	233.97	67.64	0.07	0.35	0	
Semi-degraded Meadow	0.01	0.92	0.03	2.81	3.59	55.82	178.78	1197.90	592.90	3.57	10.59	0	
Degraded Meadow	0	0.72	0.05	4.31	13.55	35.04	15.78	218.27	313.05	0.01	11.04	0	
Town	0	0.05	0	0.01	0	0.61	0.24	1.28	0.13	1.13	0.03	0	
Aeolian	0	0.15	0	0.04	0.01	0.42	0.01	2.71	3.50	0	22.89	0	
Fluvial	0	15.56	0.11	3.25	5.34	5.88	0.02	0.87	1.74	0	2.16	0	

Notes: *In general, the numbers in boldface represent an unequivocal degraded biomass from wetland system to meadow system. Within the wetland and meadow biomass, they indicate a deteriorating tendency of the wetlands and meadows system. For instance, concerning the row of “degraded wetland”, only ~58 km² of the degraded wetlands remain unchanged from 1994 to 2009, whilst ~206 km² is converted to “humid meadow” and ~105 km² is altered to “semi-degraded meadow”. In summary, rather than considering merely single landscape category, a holistic overview of the alpine landscape alterations is generated.

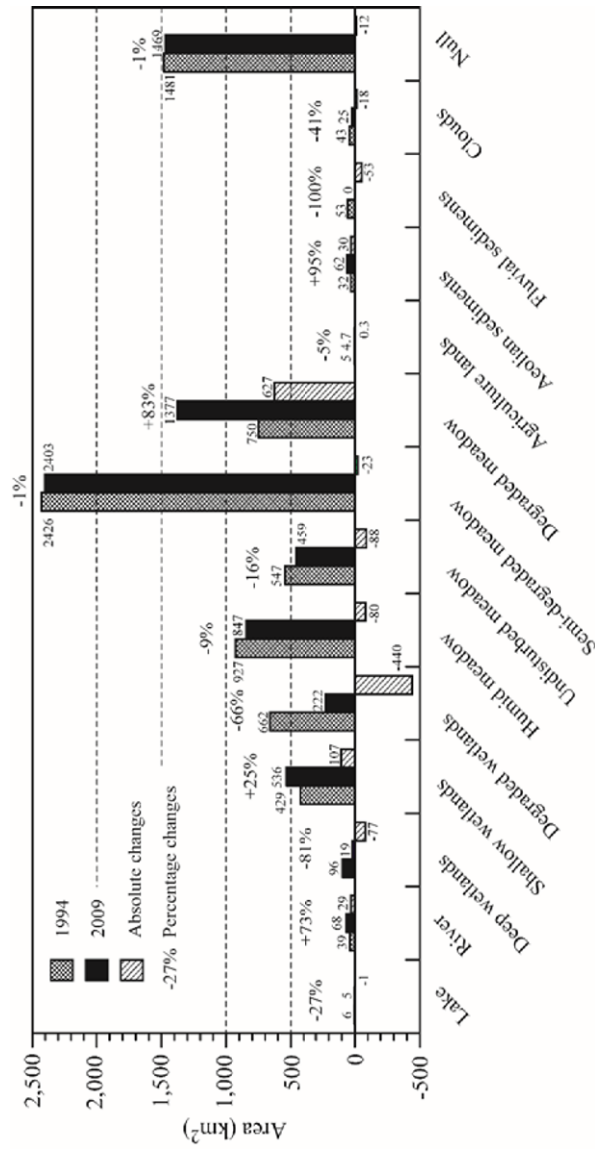


Figure 8 Variation of land-cover types in absolute values (km²) and percentages.

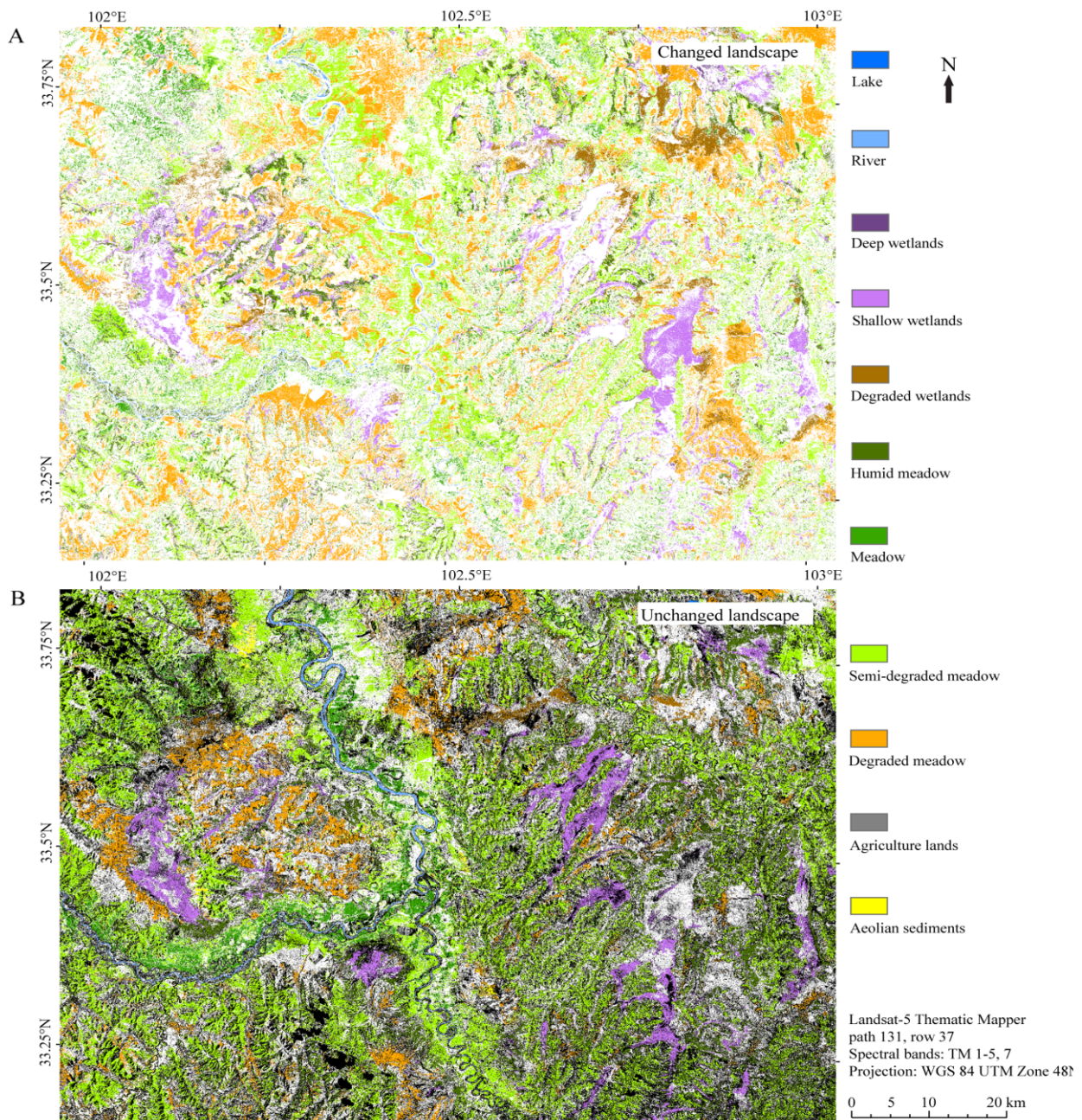


Figure 9 Spatial distribution of landscapes between the year of 1994 and 2009. Panel A delineates changed landscape whereas panel B represents unchanged landscape.

meadow and aeolian sediments, which is also marked as the most conspicuous temporal alterations of the landscapes (Table 4). Furthermore, the notable temporal tendency is the degradation from deep/shallow wetlands to degraded wetlands or humid meadow (Table 4), which may result from the artificial ditching in the rangeland and the lowering of underwater afterwards. As aforementioned, the slight

alteration of the lake and river categories may be attributed to phenological or meteorological factors, which lie out of the scope of this study. Likewise, the settlement expansion may account for the subtle variation of the townships (Table 4). These three categories will be eventually excluded from following quantitative evaluations.

To gain a quantitative view of the landscape evolution, the absolute numeric changes of area for

each landscape are represented in [Table 4](#) and [Figure 8](#). The proportion of semi-degraded meadow ranks as the largest ([Figure 8](#); [Table 4](#)). The most conspicuous change is the sharp increase of ~627 km² (ca. +83%) of degraded meadow. Concerning other landscapes, shallow wetland increases for ~107 km² (ca. +25%) and aeolian sediments (mobile dunes) have an increase of ~30 km² (ca. +95%). Considering the deterioration, a marked decrease of ~440 km² (ca. -66%) degraded wetland can be observed. Likewise, decrease of deep wetland (~78 km²; ca. -81%), humid meadow (~80 km²; ca. -9%), undisturbed meadow (~88 km²; ca. -16%), semi-degraded meadow (~23 km²; ca. -1%) and agriculture land (~0.3 km²; ca. -5%) were determined. These entire evolutions undoubtedly hint at a deteriorating tendency of the Zoige Basin landscapes, which is characterized by less proportion of preserved wetlands, meadow and agriculture lands and a considerable increasing of degraded meadow and larger areas of mobile dunes. These trends also hinder the nomadic and agriculture activities in the vicinity of Yellow River terraces due to (i) increasing of the unfavored degraded meadow, (ii) increased frequency of toxic species in the pasture biome, as well as (iii) the launching of recent policies such as fencing off the degraded pastures (e.g. [Qiu 2016](#)). The evident decrease of deep wetlands may denote a collapsing tendency of the stable humid-cold alpine meadow ecosystems and a more fragile environment being established in the Zoige Basin.

This degradation/desertification tendency of landscape is consistent with previously conducted studies encompassing [Mengsing \(1990\)](#), [Lehmkuhl \(1997\)](#), [Zeng et al. \(2003\)](#), [Dong et al. \(2010\)](#), [Hu et al. \(2015\)](#), [Bai et al. \(2013\)](#), [CX Guo et al. \(2013\)](#) and [Li et al. \(2015\)](#). In the latest report by [Hu et al. \(2015\)](#), the focus was especially devoted to aeolian sediments, three phases including increasing (1975-1990), stable (1990-2005), and decreasing (2005-2010) were identified. From 1990 to 2000, it is suggested that area of desertification has increased by 26 km², while it shows decreasing tendency thereafter ([Hu et al. 2015](#)). The ca. 30 km² increasing of the aeolian sediments in this study seems to be comparable with that of [Hu et al. \(2015\)](#). However, it needs to be noted that, our satellite image analyzed area is smaller than that of [Hu et al. \(2015\)](#). In addition, a holistic evolution

matrix comprising a whole set of land-covers ([Table 4](#); [Figure 8](#)) is still required in order to gain a reliable knowledge of land degradation and desertification in this alpine realm.

4.1.2 Spatial characteristics of landscape evolution

For the first time, apart from commonly discussed temporal changes ([Table 4](#); [Figures 7 and 8](#)), this study provides spatial characteristics ([Figure 9](#)) of the alpine landscape evolutions that are intimately coherent to the geomorphological settings, and those geomorphic factors were virtually ignored before and deserve more attention when trying to properly interpret the alpine landscape evolutions and underlying mechanisms.

As illustrated in [Figure 9B](#), the main unchanged landscapes are as follows: (i) small amounts of shallow wetlands are located on the higher terraces of Yellow and White River. (ii) Undisturbed meadow located either on the lower terraces near the river channel or in the gullies of the higher terraces, where better hydrological conditions can be approached. (iii) Humid meadow located near the shallow wetlands while unchanged deep wetlands could rarely be observed, implying degradation of the alpine biome and endangerment of the wetland ecosystems. (iv) The unchanged landscape is dominated by the semi-degraded/undisturbed meadow, suggesting an overall alpine wetland/grassland biome. The meadows are sporadically distributed in the lower terraces of rivers and gullies of higher terraces ([Figure 9B](#)), implying that, although the Zoige Basin is a humid-cold alpine meadow biome, a conspicuous tendency of deterioration can be assumed. (v) In most cases, the unchanged aeolian sediments and dunes sheets accumulate at the SE direction of the degraded meadows and lie in a relatively close distance to the channels of rivers ([Figure 9B](#)), indicating a possible origin of the silty material from the inflated/degraded meadow surface, which is subsequently transported by the NW winter monsoon to the downwind direction. In addition, the dunes at the eastern flank of the river also imply that the silty material from the fluvial sediments may also serve as provenance for the dunes and sand sheets.

As delineated in [Figure 9A](#), most conspicuous change is the increased proportion of degraded

meadow along with the mobile dunes deposited nearby. More shallow/degraded wetlands and humid meadow occurred due to the drying out wetlands. On the higher terraces of the rivers, increasing proportion of semi-degraded/degraded meadow may be converted from the degradation of the former humid/undisturbed meadows (cf. Table 4). For instance, ~593 km² semi-degraded meadows were converted into degraded meadow and ~206 km² degraded wetlands were converted to humid meadow (Table 4). In the view of topographic and geomorphological setting and due to the far reach to the groundwater, the higher terraces of the rivers might be liable to the degradation (cf. Figure 3). Therefore, the ditching and agriculture activities in the higher terraces or slopes should be treated with caution.

In summary, these entire set of evolution matrix shed light on the precedent land-cover of the degraded landscapes, delineating the most vulnerable geomorphic context in the fragile alpine ecosystem that is readily deteriorating into successor landscapes. In particular, the landscape evolution is partly constrained by the framework of relief traits (Figure 3), i.e. the slopes and higher terraces in the rangeland are more likely subject to degradation, albeit humid- and thermal-regime as well as anthropo-zoogenic factors are more likely the vital driving mechanisms.

4.2 Possible driving mechanisms of the landscape changes

From 1994 to 2009, a substantial increase of aeolian sediments at the magnitude of ca. +95% (~30 km²) was observed. Together with an array of degraded landscapes, these datasets indicate a degraded and even desertified alpine meadow ecosystem. Unlike the deserts and sandy fields in the arid and semi-arid northern China (Lu et al. 2013; Yu et al. 2013), the Zoige Basin is characterized by a humid and cold climate regime (Dong et al. 2010), rendering the possible underlying mechanisms of special interest to us. The possible driving factors are as follows.

4.2.1 Climatic factors

Meteorological parameters including precipitation and temperature are the first potential factor. Concerning the temperature, only

slightly increasing since the last decades was recorded (Li et al. 2010; Li et al. 2015) and a slight rising rate of 0.02°C/yr was reported by Bai et al. (2013). No significant decline of precipitation can be observed. The effective moisture may decrease slightly and a slightly elevated evaporation due to the temperature change is also suggested. Thus, a less favored climate condition for the preservation of wetlands together with thawing tendency of the solifluction soils might have caused the loose soils/fluvial sediments deflation (i.e. wind erosion) in the alpine meadow system. However, these slight changes in meteorological parameters are not likely to be the main driving factor for the tremendous degradation of the landscapes.

4.2.2 Anthro-po-zoogenic factors

For the pastoral ecosystem in Tibetan Plateau, a suite of anthro-po-zoogenic factors including enclosures and overgrazing were previously suggested as a more important driving mechanism for the landscape degradations (Pang et al. 2010; Hu et al. 2015; Li et al. 2015). Alternatively, at least the decadal scale of landscape changing is derived by non-climate conditions, albeit Niu et al. (2008) postulated that natural climate condition is the main influence factor for the local ecosystems. In the Tibetan Plateau, the existence of agriculture and permanent human residence was reported as early as 3600 BP (Chen et al. 2015). Palynological sequence suggests an inception of human influence before the Mid-Holocene and more intensive human impacts in the late Holocene (Schlütz and Lehmkuhl 2009; Miehe et al. 2014). In recent decades, a overloading of herbivorous e.g. yaks, sheep and horses have resulted in a tremendous overgrazing and compaction of the soil structures induced by their trampling (Table 5; Figure 6). Thus, a huge proportion of the alpine meadow was converted to semi-degraded/degraded meadow due

Table 5 Stockbreeding and over grazing of the Zoige County for different years. The data of 1990 and 1994 are cited after Lehmkuhl (1997) and 2005 after Li et al. (2008).

	Yaks	Sheep	Horse	Sheep Unit*	Over grazing %
1990	390,814	488,938	37,502	2630,518	+43.1
1994	400,000	531,000	31,000	2686,000	+45.7
2005	-	-	-	~3060,000	+64.4

Note: * Sheep Unit = yaks × 5 + sheep + horse × 5

to livestock breeding. In case of slightly higher temperature, the more fragile surface is more readily deflated and the silty material was subsequently transported to the downwind direction and accumulated as dune fields.

4.2.3 Wild mammals

In case the alpine meadow land surface is less or sparse vegetated, more mammals especially rodent may occur and they extensively damage the soil structure by digging holes. The soil system is therefore looser and the required threshold of wind speed for causing degradation is also reduced. Accompanied by the thawing of the solifluction soils, these factors have facilitated the easier and faster degradation and desertification of the alpine meadow ecosystems (cf. [Dong et al. 2010](#)).

4.2.4 Political factors

Hydrological characteristics were dramatically changed due to ditching of wetland sand peat mining in the Zoige Basin, which was launched by the local government since the 1970s ([Bai et al. 2013](#)). This policy changed the structure and configuration of the wetlands due to the lowering of the groundwater level in the whole catchment. The artificial surface runoff also intensively modulated the development of the swamps and peat bogs, which thereafter alter the behavior of the livestock in the rangeland.

In summary, rather than solely climate conditions, a suite of anthropo-zoogenic factors accompanied by interactions with slightly changed climatic factors are more likely the main driving mechanism for the landscape degradation and desertification in the alpine ecosystem of Zoige Basin. An array of tangible policies is urgent and indispensable for self-regulation and restoration of the alpine ecosystems. For instance, controlling the amount of livestock, less ditching in the rangeland and launching of a more strict nature reserve management by nearby Ruergai, Maqu and Hongyuan Counties ([Meinert and Gudehus 2013](#)) would be practical and efficacious in tracking the aforementioned goals. On the other hand, it is reported by [Lehmkuhl \(1993\)](#) that the mobile dunes near the village can be stabilized within six years by artificial planting activities, rendering its great importance of strict restoration policies with the purpose of efficient and prompt anti-degradation.

5 Conclusion

The spectral information of two Landsat-5 TM scenes (04.08.1994 and 28.07.2009, respectively) was combined with reference information obtained in the field to run supervised classifications of eight landscape types for both time steps. Subsequently, the temporal and spatial patterns of the alpine wetlands/grasslands evolutions in the Zoige Basin were analyzed based on these two classification maps. Considering single land-cover, e.g. aeolian sediments and deep wetland in 2009 scene, the merely moderate accuracy may hamper robust further explanations, rendering us to evaluate the temporal and spatial patterns rather based on a more holistic land-cover evolution matrix. Furthermore, as the land-cover classes river, fluvial sediments and townships may be readily influenced by phenological or meteorological factors, they are excluded from quantitative discussions.

In the Zoige Basin, the most conspicuous temporal change is the sharp increase of ~627 km² degraded meadow. Concerning other land-covers, shallow wetland increases for ~107 km² and aeolian sediments (mobile dunes and sand sheets) have an increase of ~30 km². These whole set of data hints at a conspicuous tendency of degradation and desertification from the year of 1994 to 2009. Apart from temporal changes, for the first time, the spatial landscape evolutions of Zoige rangeland were quantitatively determined. In this alpine realm, the land degradation is partly constrained by the framework of relief traits, namely, the slopes and higher river terraces in the rangelands are more likely liable to degradation and desertification.

Concerning the mechanisms, the slight changes in meteorological parameters are not likely to be the main driving factor for the tremendous degradation of the landscapes. In contrast, the set of anthropo-zoogenic factors encompassing enclosures, overgrazing, livestock trampling, rodent damaging and exceedingly ditching in the wetlands are assumed to be controlling factors for the Zoige Basin landscape evolution. A suite of strict protection policies are urgent and indispensable for self-regulation and restoration of the alpine ecosystem. Controlling the amount of herbivorous, less ditching in the drainage basin

and launching of a more strict nature reserve management by the adjacent Ruoergai, Maqu and Hongyuan Counties would be practical and efficacious in achieving these goals.

Acknowledgements

The study was funded by the German Research Foundation (DFG) for the fieldwork and China Scholarship Council (201306190112). We sincerely

appreciate the constructive discussion with Dr. G. Stauch regarding the methodology and language. Two anonymous reviewers are sincerely acknowledged for the constructive suggestions to improve the manuscript.

Electronic Supplementary Materials: Supplementary materials (Appendixes 1 & 2) is available in the online version of this article at <http://dx.doi.org/10.1007/s11629-016-3929-z>.

References

- Albertz J (2001) Introduction to Remote Sensing - Basics of the Aerial Satellite Image Interpretation. Darmstadt: WBG. pp 123-174. (In German)
- Bai JH, Lu QQ, Wang JJ, et al. (2013) Landscape pattern evolution processes of alpine wetlands and their driving factors in the Zoige Plateau of China. *Journal of Mountain Science* 10(1): 54-67. DOI: [10.1007/s11629-013-2572-1](https://doi.org/10.1007/s11629-013-2572-1)
- Charman DJ, Beilman DW, Blaauw M, et al. (2013) Climate-related changes in peatland carbon accumulation during the last millennium. *Biogeosciences* 10(2): 929-944. DOI: [10.5194/bg-10-929-2013](https://doi.org/10.5194/bg-10-929-2013)
- Chen FH, Bloemendal J, Zhang PZ, et al. (1999) An 800 ky proxy record of climate from lake sediments of the Zoige Basin, eastern Tibetan Plateau. *Palaeogeography, Palaeoclimatology, Palaeoecology* 151(4): 307-320. DOI: [10.1016/S0031-0182\(99\)00032-2](https://doi.org/10.1016/S0031-0182(99)00032-2)
- Chen FH, Dong GH, Zhang DJ, et al. (2015) Agriculture facilitated permanent human occupation of the Tibetan Plateau after 3,600 B.P. *Science* 347(6219): 248-250. DOI: [10.1126/science.1259172](https://doi.org/10.1126/science.1259172)
- Chen H, Wu N, Gao YH, et al. (2009) Spatial variations on methane emissions from Zoige alpine wetlands of Southwest China. *Science of the Total Environment* 407(3): 1097-1104. DOI: [10.1016/j.scitotenv.2008.10.038](https://doi.org/10.1016/j.scitotenv.2008.10.038)
- Congalton RG, Green K (2008) Assessing the accuracy of remotely sensed data: Principles and Practices. Boca Raton: CRC Press, Taylor & Francis Group. pp 55-107.
- Cui XF, Graf HF (2009) Recent land cover changes on the Tibetan Plateau: a review. *Climatic Change* 94(1): 47-61. DOI: [10.1007/s10584-009-9556-8](https://doi.org/10.1007/s10584-009-9556-8)
- Dewey JF, Shackleton RM, Chen CF, et al. (1988) The tectonic evolution of the Tibetan Plateau. *Philosophical Transactions of the Royal Society A* 327(1594): 379-413
- Dong ZB, Hu GY, Yan CZ, et al. (2010) Aeolian desertification and its causes in the Zoige Plateau of China's Qinghai-Tibetan Plateau. *Environmental Earth Science* 59(8): 1731-1740. DOI: [10.1007/s12665-009-0155-9](https://doi.org/10.1007/s12665-009-0155-9)
- Du MY, Kawashima S, Yonemura S, et al. (2004) Mutual influence between human activities and climate change in the Tibetan Plateau during recent years. *Global and Planetary Change* 41(3-4): 241-249. DOI: [10.1016/j.gloplacha.2004.01.010](https://doi.org/10.1016/j.gloplacha.2004.01.010)
- Fassnacht FE, Li L, Fritz A (2015) Mapping degraded grassland on the eastern Tibetan Plateau with multi-temporal Landsat 8 data - where do the severely degraded areas occur? *International Journal of Applied Earth Observation and Geoinformation* 42: 115-127. DOI: [10.1016/j.jag.2015.06.005](https://doi.org/10.1016/j.jag.2015.06.005)
- Guo CX, Luo F, Ding X, et al. (2013) Palaeoclimate reconstruction based on pollen records from Tangke and Riganqiao peat sections in the Zoige Plateau, China. *Quaternary International* 286: 19-28. DOI: [10.1016/j.quaint.2012.09.027](https://doi.org/10.1016/j.quaint.2012.09.027)
- Guo XJ, Du W, Wang X, et al. (2013) Degradation and structure change of humic acids corresponding to water decline in Zoige peatland, Qinghai-Tibet Plateau. *Science of the Total Environment* 445/446: 231-236. DOI: [10.1016/j.scitotenv.2012.12.048](https://doi.org/10.1016/j.scitotenv.2012.12.048)
- Harris RB (2010) Rangeland degradation on the Qinghai-Tibetan plateau: A review of the evidence of its magnitude and causes. *Journal of Arid Environments* 74(1): 1-12. DOI: [10.1016/j.jaridenv.2009.06.014](https://doi.org/10.1016/j.jaridenv.2009.06.014)
- Hu GY, Dong ZB, Lu JF, et al. (2015) The developmental trend and influencing factors of aeolian desertification in the Zoige Basin, eastern Qinghai-Tibet Plateau. *Aeolian Research* 19(Part B): 275-281. DOI: [10.1016/j.aeolia.2015.02.002](https://doi.org/10.1016/j.aeolia.2015.02.002)
- Kottek M, Greiser J, Beck C, et al. (2006) World map of Köppen-Geiger climate classification updated. *Meteorologische Zeitschrift* 15: 259-263. DOI: [10.1127/0941-2948/2006/0130](https://doi.org/10.1127/0941-2948/2006/0130)
- Lehmkuhl F (1993) "Desertification" in the Basin of Zoige (Ruoergai Plateau), Eastern Tibet. *Berliner Geographische Arbeiten* 79: 82-105. (In German)
- Lehmkuhl F (1995) Geomorphic imprints of the Holocene and late Pleistocene climate change of the Eastern Tibetan Plateau. *Göttinger Geographische Abhandlungen* 102: 1-184. (In German)
- Lehmkuhl F (1997) Areal recording of land degradation of the Zoige Basin (Eastern Tibetan Plateau) using Landsat-TM data. *Göttinger Geographische Abhandlungen* 100: 179-194. (In German)
- Lehmkuhl F, Böhner J, Stauch G (2003) Geomorphological landform and process regions in Central Asia. *Petermanns Geographische Mitteilungen* 147(H.5): 6-13. (In German)
- Lehmkuhl F, Liu SJ (1994) An outline of physical geography including Pleistocene glacier landforms of Eastern Tibet (Provinces Sichuan and Qinghai). In: Lehmkuhl F, Liu SJ (eds.), *Landscape and Quaternary climatic changes in Eastern Tibet and surroundings*. *GeoJournal* 34(1): 7-30. DOI: [10.1007/BF00813966](https://doi.org/10.1007/BF00813966)
- Lehmkuhl F, Spönemann J (1994) Morphogenetic problems of the upper Huang He drainage basin. *GeoJournal* 34(1): 31-40. DOI: [10.1007/BF00813967](https://doi.org/10.1007/BF00813967)
- Li B, Dong SC, Jiang XB, et al. (2008) Analysis on the driving factors of grassland desertification in Zoige Wetland. *Research of Soil and Water Conservation* 15(3): 112-115. (In Chinese)
- Li LS, Chen XG, Wang ZY, et al. (2010) Climate change and its regional difference over the Tibetan Plateau. *Advance in Climate Change Research* 6: 181-186. (In Chinese)
- Li ZW, Wang ZY, Brierley G, et al. (2015) Shrinkage of the Ruoergai Swamp and changes to landscape connectivity, Qinghai-Tibet Plateau. *Catena* 126: 155-163. DOI: [10.1016/j.catena.2014.10.035](https://doi.org/10.1016/j.catena.2014.10.035)
- Lillesand TM, Kiefer RW, Chipman JW (2008) Remote sensing

- and image interpretation. New York: John Wiley & Sons. pp 193-329.
- Lu HY, Yi SW, Xu ZW, et al. (2013) Chinese deserts and sand fields in Last Glacial Maximum and Holocene Optimum. *Chinese Science Bulletin* 58(23): 2775-2783. DOI: [10.1007/s11434-013-5919-7](https://doi.org/10.1007/s11434-013-5919-7)
- Mayaux P, Eva H, Brink A, et al. (2008) Remote sensing of land-cover and land-use dynamics. In: Chuvieco E (eds.), *Earth observation of global change*. Alcalá de Henares: Springer. pp 85-108.
- Meinert C, Gudehus C (2013) "From Worse to Better": Anti-Desertification Policies on the Tibetan Plateau in the Past Decades. In: *Nature, Environment and Culture in East Asia-The Challenge of Climate Change*, Leiden, Brill. pp 231-259.
- Miehe G, Miehe S, Böhner J, et al. (2014) How old is the human footprint in the world's largest alpine ecosystem? A review of multiproxy records from the Tibetan Plateau from the ecologists' viewpoint. *Quaternary Science Reviews* 86: 190-209. DOI: [10.1016/j.quascirev.2013.12.004](https://doi.org/10.1016/j.quascirev.2013.12.004)
- Niu SW, Ma LB, Zeng MM (2008) Effect of overgrazing on grassland desertification in Maqu County. *Acta Ecologica Sinica* 28(1): 145-153. (In Chinese)
- O'brian RM (2001) Subduction followed by collision: alpine and Himalayan examples. *Physics of the Earth and Planetary Interiors* 127(1-4): 277-291. DOI: [10.1016/S0031-9201\(01\)00232-1](https://doi.org/10.1016/S0031-9201(01)00232-1)
- Pang AP, Li CH, Wang X, et al. (2010) Land use/cover change in response to driving forces of Zoige Country, China. *Procedia Environmental Science* 2: 1074-1082. DOI: [10.1016/j.proenv.2010.10.119](https://doi.org/10.1016/j.proenv.2010.10.119)
- Purkis S, Klemas V (2011) *Remote sensing and global environmental change*. West Sussex: John Wiley & Sons. pp 127-271.
- Qiu J (2016) Trouble in Tibet, rapid changes in Tibetan grasslands are threatening Asia's main water supply and the livelihood of nomads. *Nature* 529(7585): 142-145. DOI: [10.1038/529142a](https://doi.org/10.1038/529142a)
- Richards JA, Jia X (2006) *Remote sensing digital image analysis*. Berlin: Springer-Verlag. pp 193-328.
- Schlütz F, Lehmkuhl F (2009) Holocene climatic change and the nomadic Anthropocene in Eastern Tibet: palynological and geomorphological results from the Nianbaoyeze Mountains. *Quaternary Science Reviews* 28(15-16): 1449-1471. DOI: [10.1016/j.quascirev.2009.01.009](https://doi.org/10.1016/j.quascirev.2009.01.009)
- Schwohengerdt RA (2007) *Remote sensing, models and methods for image processing*. Burlington: Elsevier. pp 391-473.
- Tafel A (1914) *My Tibet trip: A study tour through the Northwest China and through Inner Mongolia into the Eastern Tibet*. In: *Union Deutsche, Band 2* Stuttgart, Berlin, Leipzig. (In German)
- Xiang S, Guo RQ, Wu N, Sun SC (2009) Current status and future prospects of Zoige Marsh in Eastern Qinghai-Tibet Plateau. *Ecological Engineering* 35(4): 553-562. DOI: [10.1016/j.ecoleng.2008.02.016](https://doi.org/10.1016/j.ecoleng.2008.02.016)
- Yu KF, Hartmann K, Nottebaum V, et al. (2016) Discriminating sediment archives and sedimentary processes in the arid endorheic Ejina Basin, NW China using a robust geochemical approach. *Journal of Asian Earth Sciences* 119: 128-144. DOI: [10.1016/j.jseaes.2016.01.016](https://doi.org/10.1016/j.jseaes.2016.01.016)
- Yu KF, Lu HY, Lehmkuhl F, et al. (2013) A preliminary quantitative paleoclimate reconstruction of the dune fields of northern China during the Last Glacial Maximum and Holocene optimum. *Quaternary Science Reviews* 33(2): 293-302. (In Chinese)
- Zeng YN, Feng ZD, Cao GC (2003) Land cover change and its environmental impact in the upper reaches of the Yellow River, Northeast Qinghai-Tibetan Plateau. *Mountain Research and Development* 23(4): 353-361. DOI: [10.1659/0276-4741\(2003\)023\[0353:LCCAIE\]2.o.CO;2](https://doi.org/10.1659/0276-4741(2003)023[0353:LCCAIE]2.o.CO;2)
- Zhao Y, Tang Y, Yu ZC, et al. (2014) Holocene peatland initiation, lateral expansion, and carbon dynamics in the Zoige Basin of the eastern Tibetan Plateau. *The Holocene* 24(9): 1137-1145. DOI: [10.1177/0959683614538077](https://doi.org/10.1177/0959683614538077)
- Zhu ZD, Liu S, Di XM (1988) *Desertification and rehabilitation in China*. Lanzhou: International Centre for Education and Research on Desertification Control. p 222.